

# Experiments on hydrodynamic focusing of non coaxial sheath flows

G. Hairer, M.J. Vellekoop  
Institute of Sensor and Actuator Systems (ISAS)  
Vienna University of Technology  
Vienna, Austria  
hairer@isas.tuwien.ac.at

**Abstract**—In this paper we present experiments on chip-based non coaxial sheath flows. The uniformity of the sample flow profile along a fluidic channel and the width-limitation of hydrodynamic focusing of the sample flow are demonstrated. Additionally, the influence of varying the flow rate of the horizontal control ports on the sample flow profile is highlighted.

## I. INTRODUCTION

Hydrodynamic focusing is an attractive way to achieve a small sample flow in microfluidic devices. During hydrodynamic focusing a sample flow is squeezed between sheath flows. This technique is typically used in flow cytometry, e.g. FACS (fluorescence activated cell sorting) and coulter counters. It permits to measure, count and sort cells in a flow setup while preventing clogging of the channel and avoiding adsorption of molecules from the sample flow at the walls of the microchannel. A review of different flow cytometer systems are listed in [1] where optical and impedance analysis has been described in the field of disease diagnostics, cell/molecular biology and genetics. Different flow systems based on two-dimensional and three-dimensional focusing flow are described here. Theoretical analysis of a two-dimensional focusing stream can be found in [2] and [3]. The achieved sample flow width is roughly 5 % of the channel width used. In [3] this amounts to 20  $\mu\text{m}$ . In [4] also a device with a two-dimensionally focused stream is illustrated. The authors state that they achieved a sample width as small as 50 nm, at a channel width of 10  $\mu\text{m}$ . A three-dimensional hydro-focusing unit is demonstrated in [5]. The aim of the development of microfluidic cell analysis systems is to obtain high speed and low cost analyses of biochemical characteristics of cells keeping the sample volume low.

Hydrodynamic focusing is critical for reliable optical and impedance analysis of cells and particles. Uniformity of the sample flow over the sensing part of the channel and focusing limitations are of particular interest to achieve

reproducible measurement results of small cells or particles. In this work, experiments on non coaxial sheath flows have been carried out demonstrating uniformity of sample flow profile and the width-limitation of hydrodynamic focusing of the sample flow. Finally, the influence of varying the flow rate of the horizontal control ports on the sample flow profile is analyzed.

## II. CHIP DESIGN

Fig. 1 illustrates the principle of the non coaxial hydrodynamic focusing. A sample flow is squeezed between three sheath flows. The sample flow is moving along the channel bottom where sensors for characterizing particles and cells have been integrated. The sample liquid (diluted fluorescent dye) is vertically injected into the channel where a sheath liquid (deionized water) is flowing. After a first focusing step in the focusing section of the channel further horizontal hydrodynamic focusing is achieved with two

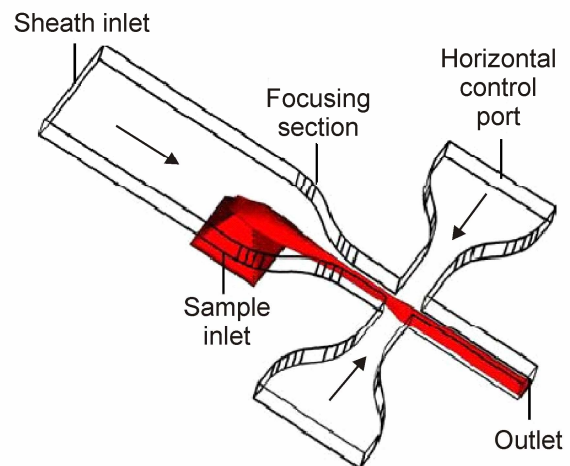


Figure 1. Schematic of non coaxial sheath flow cell: by controlling the flow rate of the sheath inlet and the horizontal control ports height and width of the sample flow can be varied.

orthogonal control ports. The sample flow is dynamically adapted by varying the flow rate ratio of the sheath inlet and the control ports to the sample flow rate. Experiments on adjustable non coaxial sheath flows have shown that the sample flow can be controlled in horizontal and vertical dimensions [6].

### III. FABRICATION AND EXPERIMENTAL SETUP

The chip was fabricated using microsystem technology. On a silicon wafer electrodes and photodiodes were integrated for impedance measurements and optical detection inside the channel. Next the wafer was anisotropic etched with a KOH water solution to achieve vertical access holes. The structure of the channel was formed by patterning a 70  $\mu\text{m}$  thick SU-8 resist. Finally the SU-8 is bonded with a glass cover slide. More details about this process can be found in [7].

For experiments a custom made device holder with o-rings was used to guarantee the fluidic connections to the syringes. The defined flow rates at the inlets were achieved with syringe pumps (kdScientific model 200 series). For the sample flow a diluted fluorescent rhodamine B dye was used and the sheath liquid was deionized water. During the experiments the chip is positioned in a fluorescence microscope (Zeiss Stemi SV11 with fluorescence equipment). A digital still camera (Sony Cybershot DSC-S75) captures images for quantitative analysis. In Fig. 2 a photo of the microfluidic device is shown where hydrodynamic focusing is examined.

### IV. MEASUREMENTS

For all experiments presented here the volumetric flow rate of the sheath inlet and the sample inlet are constantly held at 10  $\mu\text{l}/\text{min}$  and 1  $\mu\text{l}/\text{min}$ , respectively. At the inlet (region 1, Fig. 2) and the outlet (region 2, Fig. 2) of the channel (160  $\mu\text{m}$  wide and 70  $\mu\text{m}$  high) measurements are carried out. The diluted fluorescent rhodamine B was excited and the filtered fluorescence light was recorded using the

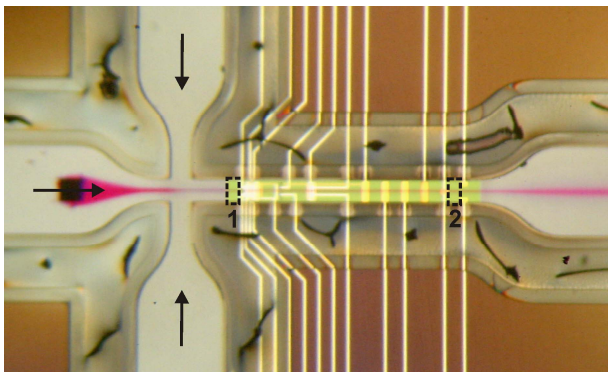


Figure 2. Experiment on hydrodynamic focusing: optical measurements were carried out at the dashed black squares 1 and 2 (distance 1.7 mm). Sample inlet: 160  $\mu\text{m}$  x 160  $\mu\text{m}$ ; channel width at inlets and outlet: 625  $\mu\text{m}$ ; channel width after focussing section: 160  $\mu\text{m}$ ; channel height: 70  $\mu\text{m}$ .

digital camera. During the measurements the flow rate of the control ports are increased in defined steps from 0 to 40  $\mu\text{l}/\text{min}$  to evaluate the uniformity of the sample flow at different focusing rates and to analyze the changes of the sample flow profile. Also the limitations of hydrodynamic focusing are experimentally verified.

### V. RESULTS AND DISCUSSION

#### A. Uniformity of the sample flow

On the left hand side of Fig. 3 fluorescence photographs of the channel at the region 1 and 2 are depicted. The images present the intensity of the primary color red, which is the emitted color of the diluted fluorescent dye. On the top of the figure the flow rate of the control ports is constantly held at 5  $\mu\text{l}/\text{min}$  and on the bottom at 40  $\mu\text{l}/\text{min}$  (sheath flow: 10  $\mu\text{l}/\text{min}$ ; sample flow: 1  $\mu\text{l}/\text{min}$ ). These images are used to analyze the profile of the stable sample flow in the channel. On the right hand side of Fig. 3 the results are depicted. The solid line represents the sample profile at region 1 and the dashed line indicates the profile of region 2 (see Fig. 2). To reduce the noise of the sample flow profile the intensity of the dye was averaged over the fluorescence image (100 adjacent lines).

To determine the height of the sample flow in the channel the intensity of the sample flow is compared to the intensity of a photograph where the channel is fully filled

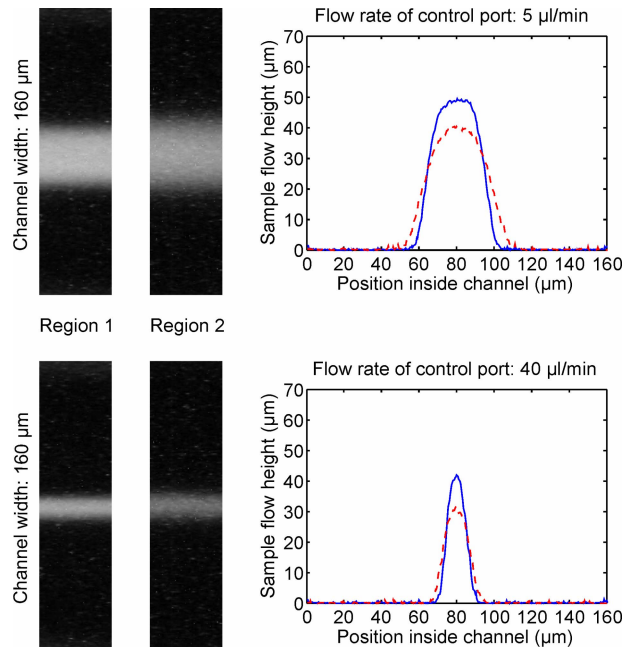


Figure 3. Measurement results of sample flow uniformity along the channel (solid line indicates region 1 and dashed line indicates region 2 as shown in Fig. 2). On the left hand side fluorescence images of the channel are illustrated and on the right hand side the evaluated results are shown. Top: The flow rate of the inlet ports are held at 10  $\mu\text{l}/\text{min}$  (sheath inlet), 1  $\mu\text{l}/\text{min}$  (sample inlet) and 5  $\mu\text{l}/\text{min}$  (control ports). Bottom: The flow rate of the control ports is increased to 40  $\mu\text{l}/\text{min}$ .

with dye. This is approved because the red color of the digital camera is not in saturation and the absorption of the light in water can be neglected due to the wavelength and the small channel height.

The measurements in Fig. 3 show the uniformity of the hydrodynamic focused sample flow over a distance of 1.7 mm. It is noticeable that the width of the sample flow spreads and the height is reduced due to diffusion effects [2].

### B. Width of the sample flow

The width of the sample flow is defined as the width of the sample at 50 % of the maximum dye intensity. On the top of Fig. 4 the width of the sample flow is depicted depending on the flow rate of the control ports. The squares illustrate the sample width on region 1 and the circles at region 2. There is a logarithmical coherence between the flow rate of the control port and the width of the sample flow. The measurements show a focusing in the range from 56  $\mu\text{m}$  to 11  $\mu\text{m}$  at region 1 and from 63  $\mu\text{m}$  to 13  $\mu\text{m}$  at region 2 at a channel width of 160  $\mu\text{m}$  by varying the flow rate of the control ports from 0 to 40  $\mu\text{l}/\text{min}$ . At high flow rate of the control ports the width reaches a limit. The control ports have hardly any influence in further reducing the width of

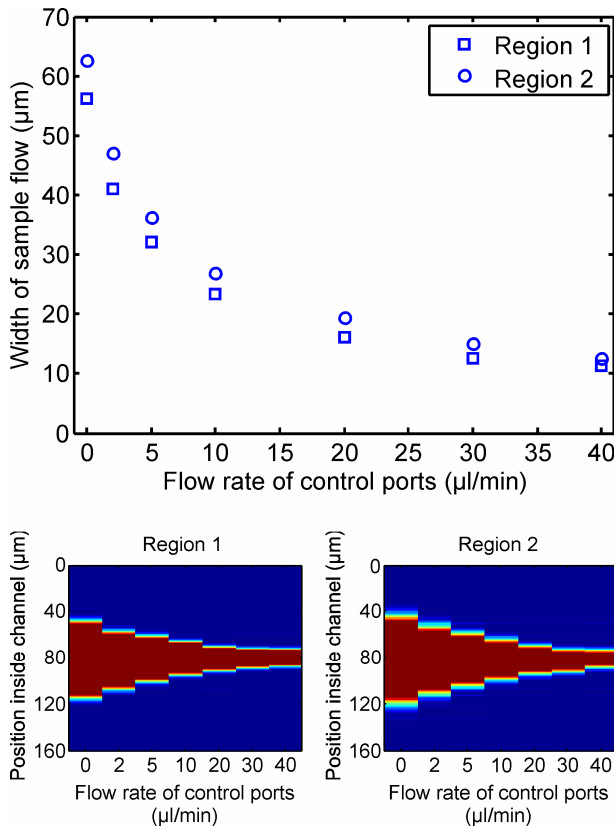


Figure 4. Top: Comparison of the width of the sample flow at region 1 and region 2 in the channel at different flow rates of the control ports (sheath inlet: 10  $\mu\text{l}/\text{min}$ ; sample inlet: 1  $\mu\text{l}/\text{min}$ ); Bottom: The position of the sample flow inside the channel (region 1 and 2) at different flow rates of the control ports.

the sample flow at higher flow rates than 40  $\mu\text{l}/\text{min}$ . The focusing limit of the sample flow in this device is 10  $\mu\text{m}$  (data not shown). The reason of the focusing limitation of non coaxial sheath flows is the low velocity of the pressure driven flow near the channel bottom (parabolic flow profile as shown in [3]).

At region 2 the width of the sample flow becomes always wider than in region 1. It can be seen the higher the flow rate of the control ports the smaller the gap between the width differences. The results clearly indicate that the diffusion effect loses ground.

In Fig. 4 at the bottom the position of the sample flow inside the channel at different flow rates of the control ports is illustrated. The focused flow always stays in the center of the channel at the beginning and the end of the small channel by applying the same flow rate at the control ports.

### C. Height of the sample flow

In Fig. 5 the influence of the height of the sample flow depending on the flow rate of the control ports is depicted. There is a linear coherence between the flow rate of the control port and the height of the sample flow. The measurements show that the height is reduced from 51  $\mu\text{m}$  to 42  $\mu\text{m}$  at region 1 and from 42  $\mu\text{m}$  to 32  $\mu\text{m}$  at region 2 at a channel height of 70  $\mu\text{m}$  by varying the flow rate of the control ports from 0 to 40  $\mu\text{l}/\text{min}$ . The flow rate of the sheath inlet and the sample inlet are constantly held at 10  $\mu\text{l}/\text{min}$  and 1  $\mu\text{l}/\text{min}$ . The tendency of the sample flow height is as follows: the higher the flow rate in the channel the lower the height of the focused sample. At higher flow rate than 40  $\mu\text{l}/\text{min}$  at the control ports the height of the sample flow still decreases. Due to the parabolic flow profile the highest velocity is in the center of the channel so the sample is squeezed to the bottom of the channel.

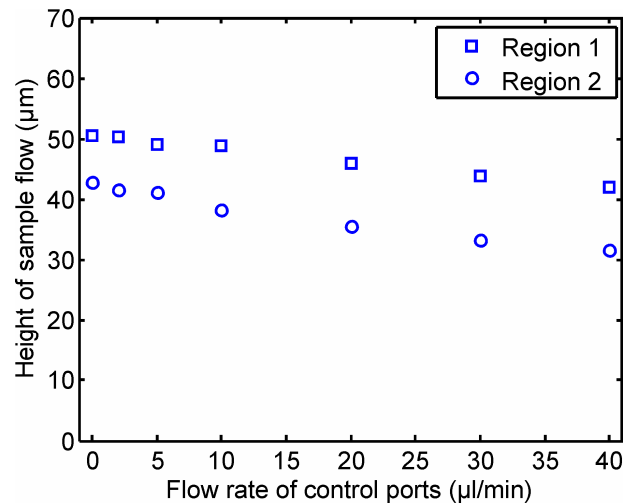


Figure 5. Comparison of the height of the sample flow at region 1 and 2 in the channel at different flow rates of the control ports (sheath inlet: 10  $\mu\text{l}/\text{min}$  and sample inlet: 1  $\mu\text{l}/\text{min}$ )

At region 2 the height of the sample flow is always lower than at region 1. The gap between the height differences of the sample flow at region 1 and 2 stays almost the same by increasing the flow rate of the control ports.

#### D. Profile of the sample flow

In Fig. 6 the reconstructed profiles of the focused sample flow at region 1 and 2 are illustrated by varying the flow rate of the control ports. Increasing the flow rate of the control ports while keeping sheath and sample flow ratio stable (10:1) the focusing of the sample increases and the height of the sample decreases. This means that the parabolic flow profile of the control ports not only reduces the width but also squeezes the sample down to the bottom, where the flow rate approaches zero. So, instead of permanently reducing width of the sample flow by increasing the flow rate of the control ports at a flow rate higher 40  $\mu\text{l}/\text{min}$  the sample flow is only squeezed more and more to the channel bottom. This experimental result demonstrates the focusing limitation for non coaxial sheath flows.

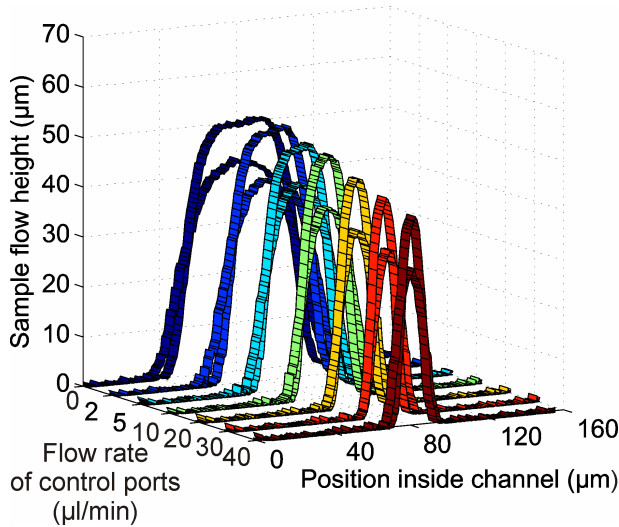


Figure 6. Comparison of the trend of the sample flow profile at the channel region 1 and 2 (width and height) by varying the flow rate of the control ports (flow rate of sheath inlet constant at 10  $\mu\text{l}/\text{min}$  and sample inlet at 1  $\mu\text{l}/\text{min}$ ).

## VI. CONCLUSIONS

In non coaxial sheath flows we have examined (i) the uniformity of the sample flow, (ii) the influence of varying the flow rate of the horizontal control ports on the sample flow profile and (iii) focusing limitations of the sample flow. The sample flow is moving along the channel bottom where sensors for characterizing particles and cells have been integrated. A high uniformity of the sample flow is needed to obtain reliable measurements. Our experiments show that uniformity can be achieved over a distance of 1.7 mm. The sample flow width and height is reduced by increasing the flow rate of the horizontal control ports. In the sample flow width a limitation is identifiable. The focusing limit on non coaxial sheath flows of this device is 10  $\mu\text{m}$  (channel width 160  $\mu\text{m}$ ). The reason for the focusing limitation is the low velocity of pressure driven flow near the channel bottom (parabolic flow profile). However, further sample flow focusing can be obtained by reducing the dimensions of the fluidic device. This is subject to current investigations.

## REFERENCES

- [1] D. Huh, W. Gu, Y. Kamotani, J. B. Grotberg, and S. Takayama, "Microfluidics for flow cytometric analysis of cells and particles", *Physiol. Meas.*, vol. 26, R73–R98, 2005.
- [2] Z. Wu, and N.-T. Nguyen, "Hydrodynamic focusing in microchannels under consideration of diffusive dispersion: theories and experiments", *Sens. Actuators B*, vol. 107, pp. 965–974, 2005.
- [3] G.-L. Lee, C.-C. Chang, S.-B. Huang, and R.-J. Yang, "The hydrodynamic focusing effect inside rectangular microchannels", *J. Micromech. Microeng.*, vol. 16, pp. 1024–1032, 2006.
- [4] J.B. Knight, A. Vishwanath, J.P. Brody, and R.H. Austin, "Hydrodynamic Focusing on a Silicon Chip: Mixing Nanoliters in Microseconds", *Physical Review Letters*, vol. 80, pp. 3863–3866, 1998.
- [5] R. Yang, D.L. Feedback, and W. Wang, "Microfabrication and test of a three-dimensional polymer hydro-focusing unit for flow cytometry applications", *Sens. Actuators A*, vol. 118, pp. 259–267, 2005.
- [6] J.H. Nieuwenhuis, J. Bastemeijer, P.M. Sarro, and M.J. Vellekoop, "Integrated flow-cells for novel adjustable sheath flows" *Lab. Chip*, vol. 3, pp. 56–61, 2003.
- [7] P. Svasek, E. Svasek, B. Lendl, and M. Vellekoop, "Fabrication of miniaturized fluidic devices using SU-8 based lithography and low temperature wafer bonding", *Sens. Actuators A*, vol. 115, pp. 591–599, 2004.